PASJ: Publ. Astron. Soc. Japan **59**, 897–903, 2007 October 25

Distance to Orion KL Measured with VERA

Tomoya HIROTA,[1,2] Takeshi BUSHIMATA,[1,3] Yoon Kyung CHOI,[1,4] Mareki HONMA,[1,2] Hiroshi IMAI,[5] Kenzaburo IWADATE,[6] Takaaki JIKE,[6] Seiji KAMENO,[5] Osamu KAMEYA,[2,6] Ryuichi KAMOHARA,[1] Yukitoshi KAN-YA,[7] Noriyuki KAWAGUCHI,[1,2,3] Masachika KIJIMA,[2] Mi Kyoung KIM,[1,4] Hideyuki KOBAYASHI,[1,3,4,6] Seisuke KUJI,[6] Tomoharu KURAYAMA,[1] Seiji MANABE,[2,6] Kenta MARUYAMA,[8] Makoto MATSUI,[8] Naoko MATSUMOTO,[8] Takeshi MIYAJI,[1,3] Takumi NAGAYAMA,[8] Akiharu NAKAGAWA,[5] Kayoko NAKAMURA,[8] Chung Sik OH,[1,4] Toshihiro OMODAKA,[5] Tomoaki OYAMA,[1] Satoshi SAKAI,[6] Tetsuo SASAO,[9,10] Katsuhisa SATO,[6] Mayumi SATO,[1,4] Katsunori M. SHIBATA,[1,2,3] Motonobu SHINTANI,[8] Yoshiaki TAMURA,[2,6] Miyuki TSUSHIMA,[8] and Kazuyoshi YAMASHITA[2]

[1]*Mizusawa VERA Observatory, National Astronomical Observatory of Japan, 2-21-1 Osawa, Mitaka, Tokyo 181-8588*
[2]*Department of Astronomical Science, Graduate University for Advanced Studies, 2-21-1 Osawa, Mitaka, Tokyo 181-8588*
[3]*Space VLBI Project, National Astronomical Observatory of Japan, 2-21-1 Osawa, Mitaka, Tokyo 181-8588*
[4]*Department of Astronomy, Graduate School of Science, The University of Tokyo, 7-3-1 Hongo, Bunkyo-ku, Tokyo 113-0033*
[5]*Faculty of Science, Kagoshima University, 1-21-35 Korimoto, Kagoshima, Kagoshima 890-0065*
[6]*Mizusawa VERA Observatory, National Astronomical Observatory of Japan, 2-12 Hoshi-ga-oka, Mizusawa-ku, Oshu, Iwate 023-0861*
[7]*Department of Astronomy, Yonsei University, 134 Shinchong-dong, Seodaemun-gu, Seoul 120-749, Republic of Korea*
[8]*Graduate School of Science and Engineering, Kagoshima University, 1-21-35 Korimoto, Kagoshima, Kagoshima 890-0065*
[9]*Department of Space Survey and Information Technology, Ajou University, Suwon 443-749, Republic of Korea*
[10]*Korean VLBI Network, Korea Astronomy and Space Science Institute, Yonsei University, 134 Shinchon-dong, Seodaemun-gu, Seoul 120-749, Republic of Korea*
tomoya.hirota@nao.ac.jp

(Received 2007 April 9; accepted 2007 May 25)

Abstract

We present the initial results of multiepoch VLBI observations of 22 GHz H_2O masers in the Orion KL region with VERA (VLBI Exploration of Radio Astrometry). With the VERA dual-beam receiving system, we carried out phase-referencing VLBI astrometry, and successfully detected the annual parallax of Orion KL to be 2.29 ± 0.10 mas, corresponding to a distance of 437 ± 19 pc from the Sun. The distance to Orion KL was determined for the first time with the trigonometric parallax method in these observations. Although this value is consistent with that previously reported, 480 ± 80 pc, which was estimated from a statistical parallax method using the proper motions and radial velocities of the H_2O maser features, our new results provide a much more accurate value with an uncertainty of only 4%. In addition to the annual parallax, we detected an absolute proper motion of the maser feature, suggesting an outflow motion powered by the radio source I along with the systematic motion of source I itself.

Key words: astrometry — ISM: individual (Orion KL) — ISM: jets and outflows — masers (H_2O) — radio lines: ISM

1. Introduction

Distance is one of the most fundamental parameters in astronomy. However, it has been difficult to measure accurate distances to stars, galaxies, and other astronomical objects without assumptions. The most reliable way to determine distance is a trigonometric parallax method, based on precise measurements of the position and motion of an object. In the 1990's, the Hipparcos satellite extensively measured annual parallaxes for more than 100000 stars with a typical precision of 1 mas level (Perryman et al. 1995, 1997), which allowed us to refine various fields of astronomy and astrophysics. Nevertheless, the distances measured with Hipparcos were limited to only within a few hundred pc from the Sun, which is far smaller than the size of the Galaxy, 15 kpc in radius.

In the last decade, phase-referencing VLBI astrometry has been developed, with which the position of a target source is measured with respect to a reference source (Beasley & Conway 1995). Using extragalactic radio sources as position references (e.g., sources listed in the International Celestial Reference Frame (ICRF) catalog: Ma et al. 1998), we can measure the absolute position of the target source, which allows us to derive its annual parallax. With recent highly precise VLBI astrometry, annual parallaxes have been successfully measured for Galactic CH_3OH maser sources at the 12 GHz band (Xu et al. 2006) and H_2O maser sources at the 22 GHz band (Kurayama et al. 2005; Hachisuka et al. 2006) with the NRAO Very Long Baseline Array (VLBA). Annual parallax measurements with VLBI have also been carried out for nonthermal radio continuum emission from young stellar objects (e.g., Lestrade et al. 1999; Loinard et al. 2005). The highest accuracy of these VLBI astrometry is reported to be

0.05 mas, which provides a powerful tool for measuring annual parallaxes with an accuracy two orders of magnitude higher than that of the Hipparcos satellite, allowing us to measure the distances of maser sources up to 2 kpc away from the Sun (Kurayama et al. 2005; Xu et al. 2006; Hachisuka et al. 2006).

In order to extend the VLBI astrometry of maser sources to the whole region of the Galaxy, we have constructed a new VLBI network in Japan, called VERA (VLBI Exploration of Radio Astrometry) (Kobayashi et al. 2003), which is the first VLBI array dedicated to phase-referencing observations. Each VERA antenna is equipped with a unique dual-beam receiving system (Kawaguchi et al. 2000; Honma et al. 2003), which enables us to observe target and reference sources within $2.^{\circ}2$ separation on the sky simultaneously, thus facilitating more efficient phase-referencing VLBI observations compared with the conventional fast-switching observations. Very recently, the first results of astrometry with VERA have been reported (e.g., Sato et al. 2007; Honma et al. 2007), demonstrating its high capability of annual parallax and absolute proper-motion measurements. The main goal of the VERA project is to reveal 3-dimensional Galactic structure and kinematics based on the accurate astrometry of hundreds of H_2O (at the 22 GHz band) and SiO (at the 43 GHz band) maser sources in the Galactic star-forming regions and late-type stars with the highest accuracy of 10 μas level (Honma et al. 2000; Kobayashi et al. 2003).

In this paper, we present initial results of annual parallax measurements of Orion KL. Because Orion KL is the nearest high-mass star-forming region located at an estimated distance of only 480 pc from the Sun (Genzel et al. 1981), it has been recognized as one of the most important objects to study high-mass star-formation processes (e.g., Genzel & Stutzki 1989). Along with its proximity to the Sun, Orion KL is known to be one of the brightest H_2O maser sources in the Galaxy, and hence it is the best test bench for the first stage of annual parallax measurements with VERA.

2. Observations and Data Analyses

Observations of H_2O masers (6_{16}–5_{23}, 22235.080 MHz) in Orion KL were carried out in 19 observing sessions from 2004 January to 2006 July with VERA. In the present work, we employed the results of a total of 16 observing sessions that were carried out under relatively good weather conditions. A typical interval of observations was 1 month, while some of them, especially in the summer season, were a few months. All of the 4 stations of VERA were used in most of the observing sessions, while only 3 stations were used in part of the sessions [2004/027, 2004/272, and 2004/333; hereafter an observing session is denoted by year/(day of the year)]. The maximum baseline length was 2270 km (see figure 1 of Petrov et al. 2007) and the typical synthesized beam size (FWMH) was 1.5 mas $\times$ 0.8 mas with a position angle of -30°.

All of the observations were made in the dual-beam mode; Orion KL and an ICRF source, J0541−0541 [α(J2000.0) = $05^{\rm h}41^{\rm m}38.^{\rm s}083385$, δ(J2000.0) = $-05^{\circ}41'49.''42839$; Ma et al. 1998; Petrov et al. 2007], were observed simultaneously. The separation angle between them was $1.^{\circ}62$. J0541−0541 was detected with a flux density of about 500 mJy in all of the observations, which was suitable as a phase reference source. The instrumental phase difference between the two beams was measured in real time during the observations, using the correlated data of random signals from artificial noise sources injected into two beams at each station (Kawaguchi et al. 2000). The typical value of the phase drift between the two beams was 3° per hour. These results were used for calibrating instrumental effects in the observed phase difference between the two sources.

Left-handed circular polarization was received and sampled with 2-bit quantization, and filtered using the VERA digital filter unit (Iguchi et al. 2005). The data were recorded onto magnetic tapes at a rate of 1024 Mbps, providing a total bandwidth of 256 MHz in which one IF channel and the rest of 15 IF channels with 16 MHz bandwidth each were assigned to Orion KL and J0541−0541, respectively. In the earlier eight observing sessions from 2004/203 to 2005/144, we used the recording system at a rate of 128 Mbps, with two IF channels of 16 MHz bandwidth each for both Orion KL and J0541−0541. A bright continuum source, J0530+1331, was observed every 1–2 hr for bandpass and delay calibration. System temperatures, including atmospheric attenuation, were measured with the chopper-wheel method (Ulich & Haas 1976) to be 100–600 K, depending on the weather conditions and the elevation angle of the observed sources. The aperture efficiencies of the antennas ranged from 45 to 52%, depending on the stations. A variation of the aperture efficiency of each antenna as a function of the elevation angle was confirmed to be less than 10%, even at the lowest elevation in the observations ($\sim 20^{\circ}$).

Correlation processing was carried out on the Mitaka FX correlator (Chikada et al. 1991) located at the National Astronomical Observatory of Japan (NAOJ) Mitaka campus. For H_2O maser lines, the spectral resolution was set to be 15.625 kHz, corresponding to a velocity resolution of 0.21 km s^{-1}. The effective velocity coverage for the H_2O maser lines, which was common for all of the observing sessions, was $\pm$40 km s^{-1} relative to the systemic velocity of Orion KL, an LSR velocity of 8 km s^{-1}.

Calibration and imaging were performed using the NRAO Astronomical Image Processing System (AIPS). At first, amplitude and bandpass calibrations were made for each of a target (Orion KL) and a reference source (J0541−0541) independently. Then, fringe fitting was made with the AIPS task FRING on the phase reference source (J0541−0541), and the phase solutions were applied to the target source (Orion KL). In addition, we adopted the results of dual-beam phase calibration measurements, as described above (Kawaguchi et al. 2000). Because the a priori delay model applied in the correlation processing was not accurate enough for precise astrometry, we calibrated the visibility phase using a more accurate delay model, based on recent achievements of geodynamics (Honma et al. 2007) in the analyses. In this model, we calibrated the fluctuation of the visibility phase caused by the Earth's atmosphere based on GPS measurements of the atmospheric zenith delay due to tropospheric water vapor.

Synthesized images were made using the AIPS task IMAGR with natural weighting. Even after the phase calibrations

described above, we found that the dynamic range of the phase-referenced images was not high enough, possibly due to a residual in the atmospheric zenith delay, as pointed out by Honma et al. (2007). To improve the quality of these images, we estimated the atmospheric zenith delay residual as a constant offset for each station, which maximized the coherence of the resultant phase-referenced image. The atmospheric zenith delay residual was derived to be 0–10 cm on average, depending on weather conditions, while it exceeded 20 cm in the worst case. As a result of this calibration, the dynamic range of each phase-referenced image increased by a factor of up to 1.5.

3. Results

Figure 1 shows the cross power spectra of the H_2O masers toward Orion KL. The H_2O maser lines were detected within the LSR velocity range of from -10 km s^{-1} to 40 km s^{-1}. We could not find high-velocity components in the LSR velocity of > 40 km s^{-1} and < -10 km s^{-1} (Genzel et al. 1981), possibly due to our narrower effective velocity coverage (from -32 to 48 km s^{-1}) and lower sensitivity.

In order to reveal the overall distribution of the H_2O masers, we at first mapped the H_2O maser features in the Orion KL region at one of the observed sessions, 2005/081, by the method adopted in usual single-beam VLBI observations. The H_2O maser features were found to be extended over the $20''$ $\times$ $30''$ region, as shown in figure 2. The distribution of the H_2O maser features is in agreement with those in Genzel et al. (1981) and Gaume et al. (1998). The number of H_2O maser features near source I, which is proposed to be a powering source of the outflow and the H_2O masers (Menten & Reid 1995; Greenhill et al. 1998), is smaller than that of the results of the NRAO Very Large Array (VLA) observations reported by Gaume et al. (1998). This is because most of the maser features near source I are resolved out with the synthesized beam of VERA, implying that their sizes are larger than a few mas (Genzel et al. 1981; Gaume et al. 1998).

Based on the H_2O maser map at the epoch of 2005/081, we searched for intense H_2O maser features whose cross power spectra observed with the Mizusawa–Iriki baseline (1267 km; see figure 1 of Petrov et al. 2007) were detected with a signal-to-noise ratio larger than 10 at all of the 16 observing epochs. We found that 10 maser features satisfied this criterion. Among them, we analyzed the data for one of the maser features at an LSR velocity of about 25 km s^{-1}, which was redshifted relative to that of the systemic velocity of Orion KL, an LSR velocity of 8 km s^{-1}, showing a relatively less significant spatial structure in the synthesized images and the closure phases during all of the observing sessions. Since the peak velocity of the maser feature was shifted systematically from 25.7 km s^{-1} to 24.5 km s^{-1} during the

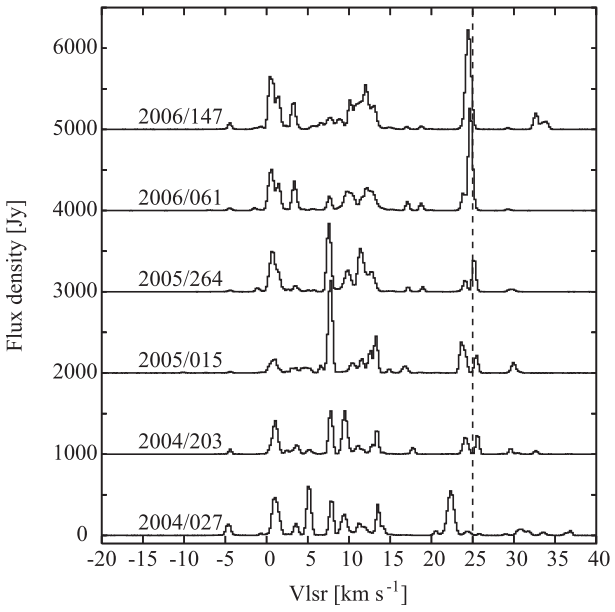

Fig. 1. Examples of scalar-averaged cross power spectra of Orion KL observed with the VERA Mizusawa–Iriki baseline (1267 km). The dashed line indicates the central velocity of the maser feature adopted for the parallax measurement in the present work at the LSR velocity of 25 km s^{-1}.

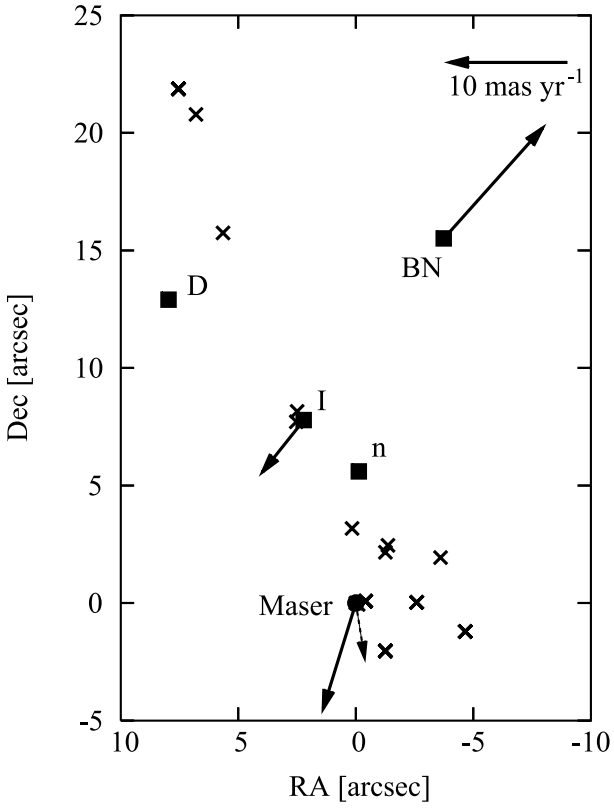

Fig. 2. Distribution of H_2O masers in Orion KL observed in the epoch of 2005/081. Crosses represent the positions of individual or groups of H_2O maser features. Filled squares and a filled circle indicate the positions of radio continuum sources (Gómez et al. 2005) and the maser feature analyzed in the present work at an LSR velocity of 24.5–25.7 km s^{-1}, respectively. Bold arrows indicate the absolute proper-motion vectors based on our study and Rodríguez et al. (2005), while the dashed arrow shows the proper motion of the maser feature with respect to source I (see text). The position offsets are with respect to the reference position [α(J2000.0) = 05^{h}35^{m}14.^{s}363600, δ(J2000.0) = $-$05°22′38.″30100].

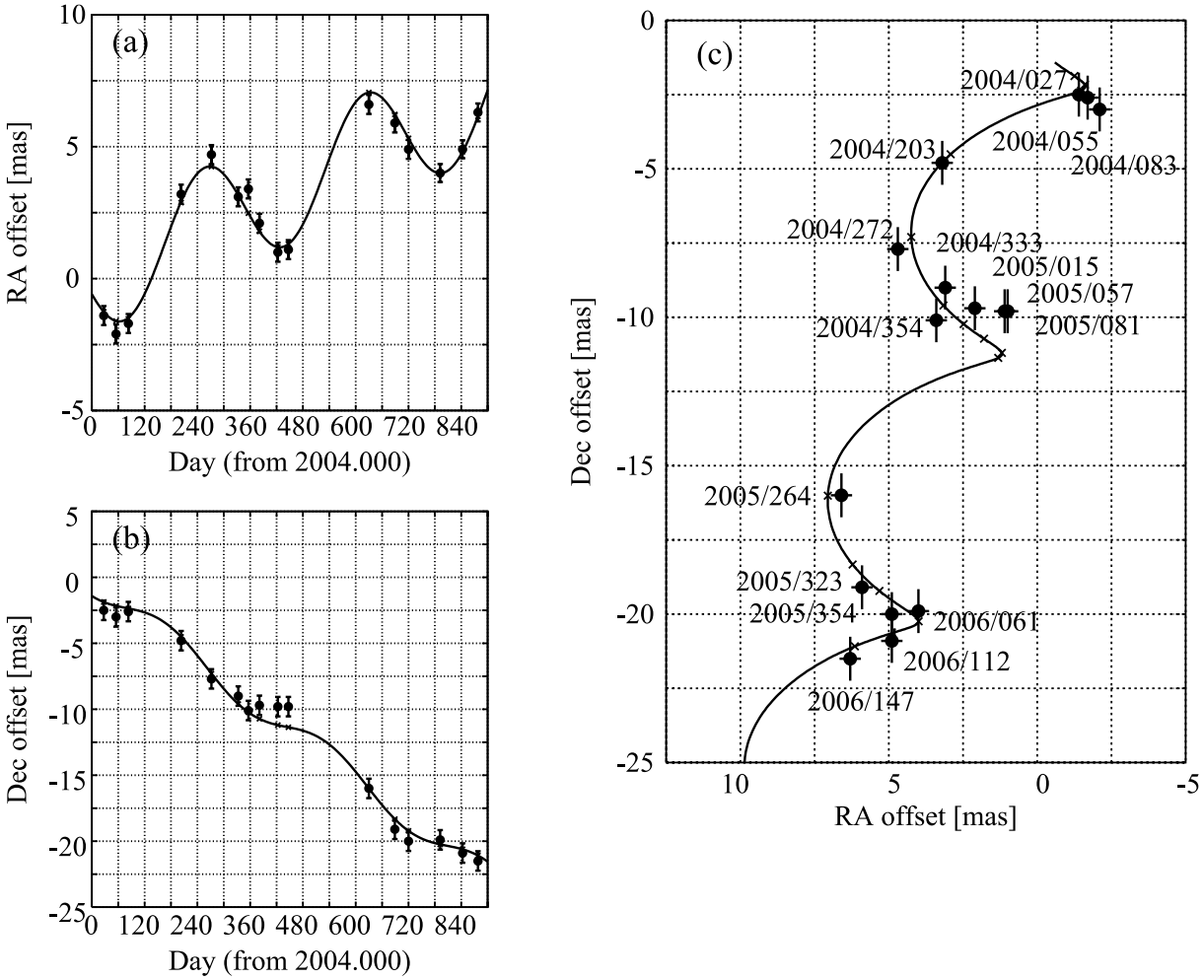

Fig. 3. Results of the position measurement of the maser feature in Orion KL. (a) Movement of the maser feature in right ascension as a function of time. (b) Same as (a) in declination. (c) Movement of the maser feature on the sky. Solid lines represent the best-fit model with the annual parallax and linear proper motion for the maser feature. Filled circles represent the observed positions of the maser feature with error bars indicating the standard deviations of the least-squares analysis, as listed in table 1 (0.36 mas in right ascension and 0.74 mas in declination). The reference position is the same as in figure 2. Observed epochs are indicated in panel (c).

observing period of 2 yr, we made images of maser spots for all of the spectral channels within the velocity range of 24.5–25.7 km s^{-1}, and determined the position of the maser feature, taking that of the peak velocity channel. Although we cannot rule out the possibility of acceleration of this maser feature, the observed velocity shift would imply a variation of its source structure. Along with the velocity shift, the flux density of the maser feature was also highly variable, as shown in figure 1. The variation of the maser feature suggested by the velocity shift and the flux variability would affect the accuracy of astrometry, even if the maser is bright, relatively stable, and with a less-significant spatial structure, as described later. Detailed analyses for all of the H_2O maser features will be reported in a forthcoming paper.

Figure 3 gives the results of our position measurements of the H_2O maser feature. As shown in figure 3, we successfully measured the movement of the H_2O maser feature for longer than 2 yr. The movement significantly deviates from a linear motion, showing a sinusoidal modulation with a period of 1 yr. This is clearly due to the annual parallax of the maser feature. In fact, the date of each peak in the sinusoidal curve is almost consistent with that predicted from the annual parallax of Orion KL. Assuming that the movement of the maser feature is the sum of the linear motion and the annual parallax, we can obtain the proper motion in right ascension, $\mu_\alpha \cos\delta$, and declination, μ_δ, the initial position in right ascension, α_0, and declination, δ_0, and the annual parallax, π, for the maser feature by a least-squares analysis.

Initially, we determined these 5 parameters simultaneously, using both right ascension and declination data. In this case, the derived annual parallax was 2.25 ± 0.21 mas, corresponding to a distance of 445 ± 42 pc; the standard deviations of the least-squares analysis in right ascension, σ_α, and in declination, σ_δ, were 0.36 mas and 0.74 mas, respectively. The larger standard deviation in declination suggests that the astrometric accuracy in the declination is significantly worse than that in the right ascension. This trend can be seen in other observations with VERA (Sato et al. 2007;

Table 1. Results of a least-squares analysis for the annual parallax and proper-motion measurements.

Parameter	Best-fit value
π	2.29(0.10) mas
$\mu_\alpha \cos\delta$	2.77(0.09) mas yr^{-1}
μ_δ	−8.97(0.21) mas yr^{-1}
σ_α	0.36 mas
σ_δ	0.74 mas

Note — Numbers in parenthesis represent the estimated uncertainties. Annual parallax, π, is derived from the right ascension data only.

Honma et al. 2007). One of the possible reasons for it is that the residual of the atmospheric zenith delay would affect the astrometric accuracy, as discussed later. Therefore, we at first determined the absolute proper motion and initial position in right ascension together with the annual parallax using only the data for right ascension. As a result, we obtained the annual parallax with higher precision to be 2.29 ± 0.10 mas, corresponding to a distance of 437 ± 19 pc. After the annual parallax was derived from the right ascension data, we estimated the absolute proper motion and initial position in declination using the data for declination. The results are summarized in table 1.

4. Discussions

4.1. Astrometric Error Sources

In the present work, we successfully measured the annual parallax of Orion KL to be 2.29 ± 0.10 mas through 2 yr-monitoring observations of the H_2O maser feature with VERA. The sinusoidal curve of the movement of the maser feature, as shown in figure 3, is almost coincident with the predicted annual parallax of Orion KL both in period (1 yr) and phase (date of the peaks in the sinusoidal curve). Therefore, the deviation from the best-fit model, which is the combination of the annual parallax and the linear proper motion of the maser feature, should be regarded as being astrometric errors in our observations, rather than due to an inappropriate model in the least-squares analysis. In this section, we will consider possible sources of these astrometric errors.

As reported previously in the literature (Kurayama et al. 2005; Hachisuka et al. 2006; Sato et al. 2007; Honma et al. 2007), it is difficult to estimate the individual error sources in the VLBI astrometry quantitatively. We therefore estimate the uncertainties in the measured position of the maser feature to be 0.36 mas and 0.74 mas in right ascension and declination, respectively, based on the standard deviation of the least-squares analysis, as listed in table 1. The standard deviations obtained here are larger than those of previous observations with VERA (Sato et al. 2007; Honma et al. 2007), especially in declination.

The most serious error source in the VLBI astrometry in the 22 GHz band is likely to be the atmospheric zenith delay residual due to tropospheric water vapor. This is caused by the difference in the optical path lengths through the atmosphere between the target and reference sources because the elevation angle of the target source is usually different from that of the reference source. According to the discussions in Honma et al. (2007), a path-length error due to an atmospheric zenith delay residual of 3 cm would cause a position error of 0.04–0.12 mas in the case of a separation angle between the target and reference source of 0.°7 at an elevation angle of 20°–90°. If we consider an extreme example, with the observed elevation angle of 20° and an atmospheric zenith delay residual of 10 cm, the position error in the observations of Orion KL and J0541−0541, with a separation angle of 1.°62, is estimated to be 0.75 mas. This value is clearly overestimated because the path-length errors should be suppressed at a higher elevation angle. Furthermore, the atmospheric zenith delay residual of 10 cm is unrealistic because we corrected such a large residual before phase-referencing imaging. Therefore, we cannot assign the cause of our position errors to only the atmospheric zenith delay residual, although it would contribute to a large part of the error source in our astrometry, especially in declination.

One of the other possibilities for the error sources in the observed position is a variation of the structure in the maser feature. With regard to this, we confirmed that the peak positions of the maser spots within the analyzed maser feature were sometimes shifted by about 0.2 mas from those of the adjacent channels. In addition, a systematic velocity shift from 25.7 km s^{-1} to 24.5 km s^{-1} was observed during the observing period of 2 yr, indicating a variation of the maser feature. Although there is no reason that the structure in the maser feature would affect the astrometric accuracy only in declination, it would be one of the major sources of errors in astrometry with the H_2O maser lines as well as the atmospheric zenith delay residual. The effect of the spatial structure of the maser feature is more significant for Orion KL than the other sources (Kurayama et al. 2005; Hachisuka et al. 2006; Sato et al. 2007; Honma et al. 2007) because the distance to Orion KL (437 pc) is nearer than the others by a factor of 5–10 (2–5 kpc). However, this effect is inversely proportional to the distance to the target source, just the same as its annual parallax. This means that the annual parallaxes of the more distant sources can be measured with almost the same precision as in the case of Orion KL, if the dominant error source in astrometry is due to a structure effect rather than the atmospheric zenith delay residual. In fact, the relative uncertainty in the annual parallax of the further source, S 269, is found to be comparable to that of Orion KL, about 4%, in the case of using only the data for right ascension (Honma et al. 2007). Further VLBI observations of maser features with shorter baselines should be able to confirm this effect, with which more extended structures of maser features are imaged.

On the other hand, the variation of the structure of the reference source, J0541−0541, would be negligible for measurements of the annual parallax and proper motion because we found no evidence for significant structure of J0541−0541 in our observations. The uncertainty in the absolute position of the reference source, J0541−0541, 0.28 mas and 0.46 mas in right ascension and declination, respectively (Ma et al. 1998), also does not affect the derived annual parallax and proper motion because this uncertainty gives only a constant offset to the position of the maser

Table 2. Results of proper-motion measurements for the observed maser feature and source I.

Source name	Absolute proper motion				Proper motion relative to source I			
	$\mu_\alpha \cos\delta$ (mas yr^{-1})	μ_δ (mas yr^{-1})	μ (mas yr^{-1})	v_t (km s^{-1})	$\mu_\alpha^{\rm I} \cos\delta$ (mas yr^{-1})	$\mu_\delta^{\rm I}$ (mas yr^{-1})	$\mu^{\rm I}$ (mas yr^{-1})	$v_t^{\rm I}$ (km s^{-1})
Maser*	2.77(0.09)	−8.97(0.21)	9.39(0.20)	19.7(0.4)†	−0.7(0.7)	−4.6(0.7)	4.6(0.7)	9.7(1.5)†
Source I*	3.5(0.7)	−4.4(0.7)	5.6(0.7)	12(2)†	0.00	0.00	0.00	0.00

Note — Numbers in parenthesis represent the estimated uncertainties.
* Absolute proper motion of source I is taken from Rodríguez et al. (2005).
† Calculated assuming the distance of 437 pc.

feature. According to discussions in Honma et al. (2007), astrometric errors in the VERA observations arising from uncertainties in the station position, delay model, and path-length errors due to ionosphere are estimated to be smaller by an order of magnitude, and hence they do not have significant effects on the astrometric accuracy. Therefore, we conclude that the major sources of our astrometric errors are due to the atmospheric zenith delay residual and variability of the structure of the maser feature.

4.2. *Annual Parallax and Distance to Orion KL*

We successfully obtained the annual parallax of Orion KL to be 2.29 ± 0.10 mas, corresponding to a distance of 437 ± 19 pc. This is the first time that the distance to Orion KL has been determined based on a trigonometric parallax method. Genzel et al. (1981) derived the distance to Orion KL to be 480 ± 80 pc by the statistical parallax method, using the proper motions and radial velocities of the H_2O maser features. Our result is consistent with that of Genzel et al. (1981), although the accuracy of our measurements is significantly improved. The most important progress in our new results is due to the geometric nature of our measurements without any assumption, unlike the statistical parallax method, in which appropriate kinematic modeling for Orion KL is required (Genzel et al. 1981). The accuracy of the annual parallax measurements in our study is limited mainly due to the atmospheric zenith delay residual and the structure of the maser feature, because it is difficult to predict and measure completely their effects in the current observational study. In principle, it will be possible to achieve much higher precision using the results of all the maser features in Orion KL, which will reduce the statistical error by a factor of $N^{-0.5}$, where N represents the number of observed maser features. This expectation will be confirmed in further analyses of the VERA observations.

4.3. *Absolute Proper Motion of the Maser Feature in Orion KL*

Along with the annual parallax measurements, we successfully detected the absolute proper motion in our phase-referencing astrometry with VERA. Figure 2 and tables 1 and 2 show the absolute proper motion of the maser feature in Orion KL. At a distance of 437 pc, the proper motion of 1 mas yr^{-1} corresponds to a transverse velocity of 2.1 km s^{-1}. The observed absolute proper motion of the H_2O maser feature (2.77 ± 0.09 mas yr^{-1} and -8.97 ± 0.21 mas yr^{-1} in right ascension and declination, respectively) corresponds to 9.39 ± 0.20 mas yr^{-1} or 19.7 ± 0.4 km s^{-1} southward.

Recently, Rodríguez et al. (2005) and Gómez et al. (2005) measured the proper motions of radio continuum sources in the Orion KL region with the VLA, as shown in figure 2 and table 2. Subtracting the proper-motion vector of source I from that of the observed maser feature, we can obtain the proper motion of the maser feature with respect to source I. As Gómez et al. (2005) have already mentioned, the precision of the absolute proper-motion measurements by Rodríguez et al. (2005) is higher than that by Gómez et al. (2005). Therefore, we adopt the proper motion of source I inferred by Rodríguez et al. (2005), 3.5 ± 0.7 mas yr^{-1} and -4.4 ± 0.7 mas yr^{-1} in right ascension and declination, respectively, in the following discussions. The proper motion of the maser feature with respect to source I is inferred to be -0.7 ± 0.7 mas yr^{-1} and -4.6 ± 0.7 mas yr^{-1} in right ascension and declination, respectively, as listed in table 2. The magnitude of the proper motion is 4.6 ± 0.7 mas yr^{-1} or 9.7 ± 1.5 km s^{-1} southward with a position angle of $-171°$, which agrees well with the direction of the outflow powered by source I. Therefore, we conclude that the absolute proper motion of the observed maser feature is the sum of outflow motion powered by source I and the systematic motion of source I itself.

However, a detailed model of the outflow powered by source I is still debatable. Greenhill et al. (1998) first proposed that the biconical high-velocity outflow traced by the SiO maser lines lies along the northwest–southeast orientation, while the low-velocity equatorial outflow traced by the H_2O maser lines exists along the northeast–southwest orientation. On the other hand, they changed the interpretation based on the recent results that the outflow is along the northeast–southwest orientation, which is perpendicular to the first model, and that the SiO maser lines trace the edge-on disk perpendicular to the outflow (Greenhill et al. 2004). We cannot distinguish these two different models in the present work because the distribution of the H_2O masers, elongated along the northeast–southwest orientation, as shown in figure 2, is consistent with both models; in addition, the proper motion of the observed H_2O maser feature is almost intermediate (southward) between the proposed outflow axes (Greenhill et al. 1998, 2004). The velocity structure in the

Orion KL region is quite complicated, as Greenhill et al. (2004) suggested, and hence further discussions about the proper motions of all the H_2O maser features are required to construct a detailed model of the outflow in the Orion KL region, which will be presented in a forthcoming paper.

We thank Dr. Yoshiaki Hagiwara for useful discussions and careful reading of the manuscript. We are also grateful to the anonymous referee for helpful comments and suggestions. We thank the staff of all the VERA stations for their assistance in observations. T. H. is financially supported by Grants-in-Aids from the Ministry of Education, Culture, Sports, Science and Technology (13640242 and 16540224).

References

Beasley, A. J., & Conway, J. E. 1995, ASP Conf. Ser., 82, 327
Chikada, Y., et al. 1991, in Frontiers of VLBI, ed. H. Hirabayashi, M. Inoue, & H. Kobayashi (Tokyo: Universal Academy Press), 79
Gaume, R. A., Wilson, T. L., Vrba, F. J., Johnston, K. J., & Schmid-Burgk, J. 1998, ApJ, 493, 940
Genzel, R., Reid, M. J., Moran, J. M., & Downes, D. 1981, ApJ, 244, 884
Genzel, R., & Stutzki, J. 1989, ARA&A, 27, 41
Gómez, L., Rodríguez, L. F., Loinard, L., Lizano, S., Poveda, A., & Allen, C. 2005, ApJ, 635, 1166
Greenhill, L. J., Gwinn, C. R., Schwartz, C., Moran, J. M., & Diamond, P. J. 1998, Nature, 396, 650
Greenhill, L. J., Reid, M. J., Chandler, C. J., Diamond, P. J., & Elitzur, M. 2004, IAU Symp., 221, 155
Hachisuka, K., et al. 2006, ApJ, 645, 337
Honma, M., Kawaguchi, N., & Sasao, T. 2000, Proc. SPIE, 4015, 624
Honma, M., et al. 2003, PASJ, 55, L57
Honma, M., et al. 2007, PASJ, 59, 889
Iguchi, S., Kurayama, T., Kawaguchi, N., & Kawakami, K. 2005, PASJ, 57, 259
Kawaguchi, N., Sasao, T., & Manabe, S. 2000, Proc. SPIE, 4015, 544
Kobayashi, H., et al. 2003, ASP Conf. Ser., 306, 367
Kurayama, T., Sasao, T., & Kobayashi, H. 2005, ApJ, 627, L49
Lestrade, J.-F., Preston, R. A., Jones, D. L., Phillips, R. B., Rogers, A. E. E., Titus, M. A., Rioja, M. J., & Gabuzda, D. C. 1999, A&A, 344, 1014
Loinard, L., Mioduszewski, A. J., Rodríguez, L. F., González, R. A., Rodríguez, M. I., & Torres, R. M. 2005, ApJ, 619, L179
Ma, C., et al. 1998, AJ, 116, 516
Menten, K. M., & Reid, M. J. 1995, ApJ, 445, L157
Perryman, M. A. C., et al. 1995, A&A, 304, 69
Perryman, M. A. C., et al. 1997, A&A, 323, L49
Petrov, L., Hirota, T., Honma, M., Shibata, K. M., Jike, T., & Kobayashi, H. 2007, AJ, 133, 2487
Rodríguez, L. F., Poveda, A., Lizano, S., & Allen, C. 2005, ApJ, 627, L65
Sato, M., et al. 2007, PASJ, 59, 743
Ulich, B. L., & Haas, R. W. 1976, ApJS, 30, 247
Xu, Y., Reid, M. J., Zheng, X. W., & Menten, K. M. 2006, Science, 311, 54